Influence of the self-energy diagrams on the solutions of a scalar Bethe-Salpeter equation

Bing An Li*
Stanford Linear Accelerator Center, Stanford University, Stanford, California 94305

Ting Chang Hsien
Institute of High Energy Physics, Academia Sinica, Beijing, People's Republic of China

Suh Yan, Tien Lun Chen, Ching Zhu Yang, and Jing Fa Lu
Department of Physics, Nankai University, People's Republic of China
(Received 29 January 1980)

The influence of self-energy diagrams on solutions of the Bethe-Salpeter equation is studied by taking a $g\phi_1^*(x)\phi_1(x)\phi_2(x)$ interaction in the ladder approximation. The results show that for ground-state solutions the self-energy diagrams will diminish the eigenvalues and alter the wave functions slightly. However, for the excited states and antisymmetric solutions, the influence of the self-energy diagrams is considerable, and completely alters the properties of the solutions. Their wave functions look like a δ function and their eigenvalues are independent of the binding energy and the quantum numbers. The results also show that the infrared behavior of the self-energy diagrams is very important for the solutions of the equation, and that the solutions from the ladder approximation are meaningful only in the loosely bound cases. As the binding becomes tight, the contribution from the self-energy diagrams becomes important.

I. INTRODUCTION

During recent years interest in bound states has increased. We can use the Bethe-Salpeter (BS) equation to describe bound states. In general, the BS equation becomes very complicated in the case of strong interactions. For example, the scalar BS equation has the form

$$\Delta^{-1}(p_1)\Delta^{-1}(p_2)\chi(p) = \int G(P,p,p')\chi(p')d^4p', \qquad (1.1)$$

where

$$(2\pi)^4\delta^4(p_1+p_2-P)\chi(p) = \int d^4x_1 d^4x_2 e^{-ip_1x_1-ip_2x_2} \times\langle 0|T\{\phi_1(x_1)\phi_1^*(x_2)\}|a\rangle, \qquad (1.2)$$

$$p_1 = p+\tfrac{1}{2}P, \quad p_2 = -p+\tfrac{1}{2}P, \quad \Delta^{-1}(p) = i(p^2+m^2).$$

P_μ is the center-of-mass four-momentum of the bound state. p_μ is the relative four-momentum; m is the mass of the particles (equal-mass particles by assumption) which constitute the bound states. $G(P,p,p')$ is the integral kernel determined by four-point irreducible Feynman diagrams as well as by self-energy diagrams. Up until now nobody has been able to add up all the diagrams in order to solve the equation. Thus, some lower-order diagrams are taken to solve the equation. The ladder approximation is often used.

In 1954, Wick[1] and Cutkosky[2] studied the solutions of a scalar BS equation in the ladder approximation. Their results led to some understanding of the equation in this approximation. They found the existence of some abnormal solutions in the case of strong coupling. The abnormal states do not correspond to the solutions of the nonrelativistic equation. The nonrelativistic bound states are in three-dimensional space. The quantum numbers are the radial quantum number and the orbital angular momentum. However, relativistic bound states are in four-dimensional space. The abnormal states correspond to the quantization of four-dimensional space-time. Many people have studied this problem.[3] There are some different points of view. But up to now no physical states have been found which correspond to the abnormal solutions. Blankenbecler and Sugar[4] have discussed the importance of satisfying unitarity conditions in the equation. Levine and Wright[5,6] have solved a scalar BS equation. They found that in the inelastic region the unitarity condition

$$\sigma_{\text{tot}} \geq \sigma_{\text{elastic}} \qquad (1.3)$$

can be violated if only ladder diagrams are taken in the integral kernel. However, if the contribution of self-energy diagrams is included, then the unitarity condition is satisfied in the inelastic scattering region. We know that if the unitarity condition is violated some unphysical effects will appear.

In this paper we want to discuss what changes will occur in the bound-state solutions if the self-energy diagrams are included in the integral kernel.

This paper is divided into six sections. In Sec. II we discuss the equation and the method used to solve the equation. In Sec. III the solutions with-

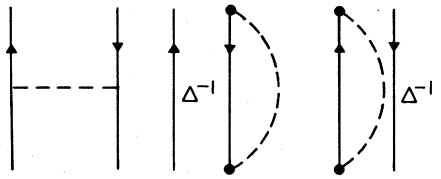

FIG. 1. Ladder diagram and self-energy diagrams in the integral kernel.

out considering the contribution of self-energy diagrams are given and compared with those obtained by using other methods. In Sec. IV the solutions with self-energy diagrams are given. In Sec. V the wave functions which are obtained are discussed. Section VI is a brief discussion of the results obtained by us.

II. THE EQUATION AND THE METHOD

For the sake of simplicity we still discuss a scalar BS equation. The interaction is chosen to be

$$\mathcal{H}_i(x) = g\phi_1^*(x)\phi_1(x)\phi_2(x)\,, \tag{2.1}$$

where $\phi_1(x)$ is a complex scalar field whose mass is denoted by m. $\phi_2(x)$ is a neutral scalar field whose mass is denoted by μ. The kernel G is taken up to second-order diagrams in the coupling constant in Fig. 1. By using these diagrams (Fig. 1) the four-point Green's function is denoted in Fig. 2. Each bubble of Fig. 2 is composed of self-energy diagrams as shown in Fig. 3.

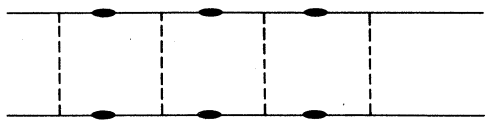

FIG. 2. Ladder diagrams with self-energy diagrams.

When second-order diagrams are included in the kernel, the integral kernel in the BS equation has the form

$$G(P,p,p') = \frac{i\lambda}{\pi^2}\frac{1}{(p-p')^2+\mu^2} - \lambda h(p)(p_1^2+m^2)(p_2^2+m^2)\delta^4(p-p')\,, \tag{2.2}$$

where

$$h(p) = \int_{(m+\mu)^2}^{\infty} \frac{(p_1^2+m^2)[\sigma^2-(m+\mu)^2]^{1/2}[\sigma^2-(m-\mu)^2]^{1/2}}{\sigma^2(\sigma^2-m^2)^2(p_1^2+\sigma^2-i\epsilon)}\,d\sigma^2 + \int_{(m+\mu)^2}^{\infty} \frac{(p_2^2+m^2)[\sigma^2-(m+\mu)^2]^{1/2}[\sigma^2-(m-\mu)^2]^{1/2}}{\sigma^2(\sigma^2-m^2)^2(p_2^2+\sigma^2-i\epsilon)}\,d\sigma^2\,. \tag{2.3}$$

The expression $h(p)$ of the self-energy diagrams is obtained by using the method of the spectral function. Renormalization has been carried out.

Substituting formula (2.2) into Eq. (1.1) and after Wick rotation, the equation can be written in the form

$$(p_1^2+m^2)(p_2^2+m^2)\chi(p) = \frac{\lambda}{\pi^2}\int \frac{\chi(p')d^4p'}{(p-p')^2+\mu^2} + \lambda h(p)(p_1^2+m^2)(p_2^2+m^2)\chi(p). \tag{2.4}$$

Now both momentum p and p' are in Euclidean space. In the rest frame of the bound state, by using the rotational invariance of the equation, we single out the three-dimensional harmonics corresponding to the orbital motion, and discuss the case in which the orbital quantum numbers are l and m:

$$\chi(p) = \frac{1}{|\vec{p}|}f_l(|\vec{p}|,p_4)Y_{lm}(\theta,\phi)\,. \tag{2.5}$$

Substituting formula (2.5) into Eq. (2.4), we obtain

$$\psi_l(p) = \frac{2\lambda}{\pi}\int_{-\infty}^{+\infty}dp_4'\int_0^{\infty}d|\vec{p}'|\frac{Q_l(a)}{L(p)L(p')}\psi_l(|\vec{p}'|,p_4') + \lambda h(p)\psi_l(p)\,, \tag{2.6}$$

where $Q_l(a)$ is the Legendre function of the second kind and

$$a = \frac{(p_4-p_4')^2+|\vec{p}|^2+|\vec{p}'|^2+\mu^2}{2|\vec{p}||\vec{p}'|}\,,$$
$$\psi_l(p) = L(p)f_l(p)\,,$$
$$L^2(p) = (|\vec{p}|^2+p_4^2+1-\eta^2)^2+4\eta^2p_4^2\,, \tag{2.7}$$
$$\eta = \frac{M}{2m} = \frac{2m+B}{2m}\,,$$

where B is the binding energy, M is the rest mass of the bound state, and η is a parameter which is related to the binding energy. All the quantities in Eq. (2.6) are in units of m, and hence are dimensionless.

Equation (2.6) is a two-dimensional integral

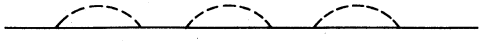

FIG. 3. Bubble diagrams of Fig. 2.

equation in Euclidean space and is invariant under the transformation $p_4 \rightarrow -p_4$. Using this symmetry, the equation can be rewritten as

$$\psi_l^{\pm}(p) = \lambda h(p)\psi_l^{\pm}(p) + \lambda \int_0^{\infty} dp_4' \int_0^{\infty} d|\vec{p}'| K^{\pm}(p,p')\psi_l^{\pm}(p'), \quad (2.8)$$

where

$$K^{\pm}(p,p') = \frac{2}{\pi} \frac{Q_l(a(p_4)) \pm Q_l(a(-p_4))}{L(p)L(p')}. \quad (2.9)$$

Because $h(p)$ is an even function of the variable p_4, we have

$$\psi_l^{\pm}(|\vec{p}|, -p_4) = \pm \psi_l^{\pm}(|\vec{p}|, p_4). \quad (2.10)$$

It is obvious that no nonrelativistic approximation exists for $\psi_l^-(p)$; hence, it is the anomalous solution. In the following calculation, ψ_l^+ and ψ_l^- are solved separately.

Now we introduce the following new variables:

$$|\vec{p}| = \frac{1+x}{1-x}, \quad p_4 = \frac{1+y}{1-y}, \quad (2.11)$$

then the regions of the integration of new variables x and y become $(-1,1)$. The method of Gaussian quadrature is used to solve the integral equation. We obtain a set of algebraic equations

$$\lambda^{-1}\chi_{ij}^{\pm} = h_{ij}\chi_{ij}^{\pm} + \sum_{l,m=1}^{N} A_{ij,lm}\chi_{lm}^{\pm}, \quad (2.12)$$

where

$$A_{ij,lm}^{\pm} = \frac{2(\omega_i\omega_j\omega_l\omega_m)^{1/2}}{(1-x_i)(1-y_j)(1-x_l)(1-y_m)} K_{ij,lm}^{\pm},$$
$$\chi_{ij}^{\pm} = \frac{(\omega_i\omega_j)^{1/2}}{(1-x_i)(1-y_j)}\psi_{ij}^{\pm}. \quad (2.13)$$

The ω_i's are the weights of Gaussian integration. Equation (2.12) is a set of coupled algebraic equations which is solved numerically on a DJS-8 computer.

III. SOLUTIONS WITHOUT CONSIDERING THE SELF-ENERGY DIAGRAMS

In order to examine the influence of the self-energy diagrams on the solutions and check the method used to solve the equation, we first solve the equation without considering the self-energy diagrams. After removing the self-energy term $h(p)$ from Eq. (2.8), the equation becomes a standard Fredholm integral equation whose properties are well known. In the corresponding algebraic equation (2.12), after removing the term corresponding to the self-energy diagrams, we use ten Gaussian points and solve the eigenvalues and eigenfunctions of a 100×100 determinant. The parameters η and μ are taken to be

$$\eta = 0.0, 0.2, 0.4, 0.6, 0.9, 0.99,$$
$$\mu = 1, 0.1, 0.01.$$

The symmetric and antisymmetric ground states and several excited states are solved for the S and P waves. The eigenvalues for $\mu = 1$ are shown in Table I, in which $\lambda_{l,n}^{\pm}$ are the eigenvalues corresponding to the symmetric and antisymmetric wave functions with the orbital angular momentum l and quantum number n, respectively, where n is labeled according to the magnitude of the eigenvalues from 0 on. The λ^*'s were obtained by Zur Linden and Mitter[7] by expanding the wavefunction in the four-dimensional spherical harmonics and solving the resultant one-dimensional integral

TABLE I. Eigenvalues without considering self-energy diagrams at $\mu = 1$.

η	0.0	0.2	0.4	0.6	0.9	0.99
$\lambda_{0,0}^{+}$	3.416	3.342	3.114	2.717	1.665	1.010
λ^{*}	3.419	3.344	3.115	2.718	1.665	1.014
$\lambda_{0,1}^{+}$	16.69	16.40	15.52	13.90	9.79	7.07
$\lambda_{0,2}^{+}$	45.02	44.44	42.67	39.41	29.72	23.04
$\lambda_{1,0}^{+}$	16.30	16.02	15.17	13.68	9.80	7.73
$\lambda_{1,1}^{+}$	46.18	45.57	43.51	39.89	30.43	25.05
$\lambda_{1,2}^{+}$	85.82	85.07	82.81	79.01	68.17	59.16
$\lambda_{0,0}^{-}$	16.33	16.20	15.80	15.12	13.51	12.87
$\lambda_{0,1}^{-}$	46.45	46.09	44.98	43.09	38.60	36.79
$\lambda_{1,0}^{-}$	73.82	72.97	70.35	65.60	51.71	42.21
$\lambda_{1,1}^{-}$	109.4	108.4	106.4	102.3	91.13	84.91

TABLE II. Eigenvalues without considering self-energy diagrams at $\mu = 0.1$.

η	0.0	0.2	0.4	0.6	0.9	0.99
$\lambda^{+}_{0,0}$	2.008	1.946	1.757	1.434	0.608	0.185
$\lambda^{+}_{0,1}$	6.04	5.85	5.28	4.31	1.86	0.63
$\lambda^{+}_{0,2}$	11.65	11.38	10.55	9.00	3.79	1.40
$\lambda^{+}_{1,0}$	5.95	5.76	5.20	4.22	1.82	0.61
$\lambda^{+}_{1,1}$	11.56	11.19	10.10	8.31	3.64	1.29
$\lambda^{+}_{1,2}$	17.60	17.30	16.38	13.59	6.35	2.42
$\lambda^{-}_{0,0}$	5.93	5.81	5.45	4.81	3.08	2.19
$\lambda^{-}_{0,1}$	11.55	11.31	10.59	9.29	5.69	3.95

equation by using 32 Gaussian points. From Table I we see that λ^{*} agrees with $\lambda^{+}_{0,0}$ obtained by us up to the third significant figure. Pagnamenta[8] solved the equation (without self-energy diagrams) by using 12 Gaussian points and obtained $\lambda^{+}_{0,0} = 3.4182$ (for $\eta = 0.0$), which agrees with our result also up to the third significant figure. Schwartz[9] exploited the variational method to calculate $\lambda^{+}_{0,1}$, $\lambda^{+}_{1,0}$, and $\lambda^{-}_{0,0}$, and his results agree with ours up to the second or third significant figure. The eigenvalues corresponding to $\mu = 0.1$ and 0.01 are given in Tables II and III, from which we see that for fixed η, λ decreases as μ decreases; i.e., the spectrum of λ becomes denser as μ decreases. In order to examine the stability of the results obtained, we have also used eight Gaussian points to solve the equation and compared the results with the above-mentioned ones in various references. It turns out that the eigenvalues tabulated in these tables remain unchanged up to the third significant figure for the ground state, and up to the second or third significant figure for the excited states.

TABLE III. Eigenvalues without considering self-energy diagrams at $\mu = 0.01$.

η	0.0	0.2	0.4	0.6	0.9	0.99
$\lambda^{+}_{0,0}$	1.830	1.773	1.598	1.296	0.525	0.111
$\lambda^{+}_{0,1}$	4.88	4.72	4.24	3.42	1.31	0.22
$\lambda^{+}_{0,2}$	7.29	7.14	6.68	5.55	1.98	0.39
$\lambda^{+}_{1,0}$	4.68	4.53	4.06	3.26	1.24	0.23
$\lambda^{+}_{1,1}$	7.86	7.62	6.91	5.64	2.11	0.31
$\lambda^{+}_{1,2}$	9.02	8.83	8.28	7.08	2.51	0.56
$\lambda^{-}_{0,0}$	4.44	4.35	4.05	3.51	1.92	0.67
$\lambda^{-}_{0,1}$	7.45	7.29	6.77	5.74	2.86	0.88
$\lambda^{-}_{1,0}$	9.01	8.82	8.22	7.01	3.23	0.86

TABLE IV. Eigenvalues considering self-energy diagrams at $\mu = 1$.

η	0.0	0.2	0.4	0.6	0.9	0.99
$\lambda'^{+}_{0,0}$	2.282	2.262	2.196	2.053	1.484	0.97
$\lambda'^{+}_{0,1}$	2.39	2.39	2.39	2.39	2.39	2.39
$\lambda'^{+}_{0,2}$	2.40	2.40	2.40	2.40	2.40	2.40
$\lambda'^{-}_{0,0}$	2.39	2.38	2.37	2.38	2.37	2.37
$\lambda'^{\pm}_{1,0}$	2.39	2.39	2.39	2.39	2.39	2.39

IV. INFLUENCE OF THE SELF-ENERGY DIAGRAMS

When the self-energy diagrams are taken into consideration, we have to solve Eq. (2.21), which contains the diagonal terms

$$h_{ij}\chi^{\pm}_{ij}.$$

In solving the equation, ten Gaussian points are still used. The eigenvalues obtained are given in Tables IV–VI. From these results we make the following conclusions:

(1) For $\mu = 1$, there exists a ground-state solution of the symmetric wave function whose eigenvalues are lower than that when the contribution of the self-energy diagram is neglected (30% lower for $\eta = 0$). This difference diminishes as η increases, and for $\eta \to 1$. They approach the same limit which shows that the contribution of the self-energy diagrams is small for loosely bound states ($\eta \sim 1$). This can also be seen from Fig. 4. This result agrees with Blankenbecler and Levine.[5,6]

(2) For $\mu = 1$, all antisymmetric solutions and symmetric excited solutions are degenerate and the eigenvalues are independent of η. In this case the calculated results show that

$$h(p)\chi(p) \gg \frac{1}{\pi^2}\frac{1}{(p_1^2+1)(p_2^2+1)} \times \int \frac{\chi(p')d^4p'}{(p-p')^2+\mu^2}.$$

Hence, the contribution of the self-energy diagrams is dominant. In this case the eigenvalues are equal to the inverse of the maximum of $h(p)$. For

TABLE V. Eigenvalues considering self-energy diagrams at $\mu = 0.1$.

η	0.0	0.2	0.4	0.6	0.9	0.99
$\lambda'^{+}_{0,0}$	0.3317	0.3317	0.3317	0.3317	0.3317	0.1714
$\lambda'^{+}_{0,1}$	0.332	0.332	0.332	0.332	0.332	0.332

TABLE VI. Eigenvalues considering self-energy diagrams at $\mu = 0.01$.

η	0.0	0.2	0.4	0.6	0.9	0.99
$\lambda'^{+}_{0,0}$	0.1378	0.1378	0.1378	0.1378	0.1378	0.0889
$\lambda'^{+}_{0,1}$	0.1378	0.1378	0.1378	0.1378	0.1378	0.1378
$\lambda'^{-}_{0,0}$	0.1378	0.1378	0.1378	0.1378	0.1378	0.1378
$\lambda'^{-}_{0,1}$	0.1379	0.1379	0.1379	0.1379	0.1379	0.1379

$\mu = 1$, we obtain

$$h(p)_{\max} = 0.417 = \lambda^{-1},$$

hence

$$\lambda = 2.39.$$

It is the same as the calculated results. Since the terms corresponding to the self-energy diagrams control the solution of the equation, the discrete spectrum does not exist and only the continuous spectrum exists. For the ground state of the antisymmetric wave function, its integral kernel K^{-} is small. This kernel causes the larger value $\lambda^{-}_{0,0} = 16.33$ if self-energy diagrams are ignored. For the excited states of both symmetric and antisymmetric wave functions there are some zero points in the wave functions which cause the integral

$$\int \frac{\chi(p')d^4p'}{(p-p')^2+\mu^2} \quad \text{for the excited states}$$

to be small. This can be seen from the large values of $\lambda^{+}_{0,1}$, $\lambda^{+}_{0,2}$, $\lambda^{+}_{1,0}$, $\lambda^{+}_{1,1}$, $\lambda^{+}_{1,2}$, $\lambda^{-}_{0,1}$, $\lambda^{-}_{1,0}$, and $\lambda^{-}_{1,1}$ (Table I). These results show that the integrals are small in the case of the ground state of the antisymmetric wave function and the excited states. Thus, the self-energy term controls the solution of the equation in these cases.

(3) For $\mu = 0.1$ and 0.01 all the eigenvalues of the

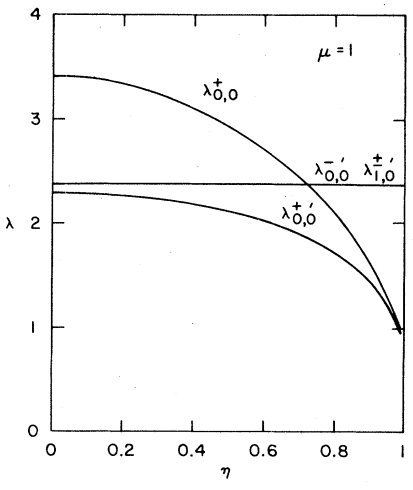

FIG. 4. Eigenvalues at $\mu = 1$. $\lambda^{+}_{0,0}$ is the eigenvalue of the ground state without considering self-energy diagrams. $\lambda^{-\prime}_{0,0}$, $\lambda^{\pm\prime}_{1,0}$, and $\lambda^{+\prime}_{0,0}$ are eigenvalues considering self-energy diagrams.

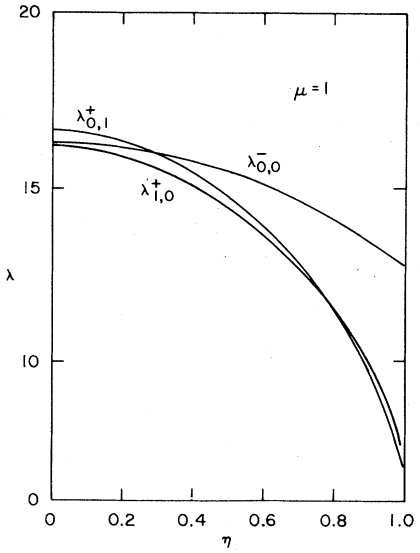

FIG. 5. Eigenvalues without considering self-energy diagrams at $\mu = 1$.

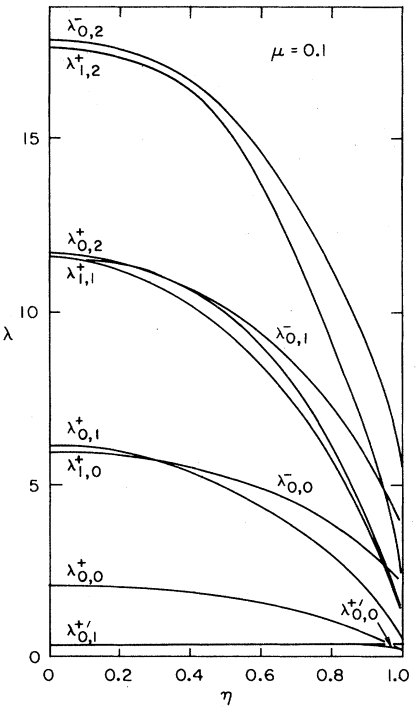

FIG. 6. Eigenvalues at $\mu = 0.1$.

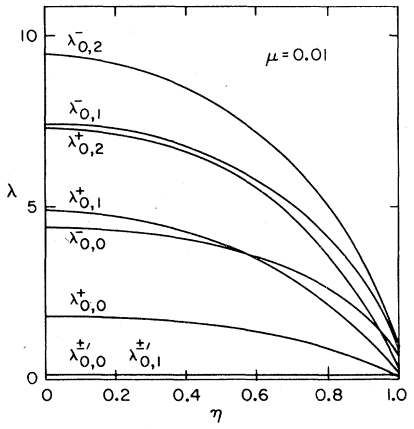

FIG. 7. Eigenvalues at $\mu = 0.01$.

ground state corresponding to $\eta \leq 0.9$ are constant, i.e., $1/h_{\max}$. Only for loosely bound states ($\eta > 0.99$) can the different eigenvalues be found and the ground state of the symmetric wave function exist. These eigenvalues approach the values without considering self-energy diagrams. The calculated results show that as μ gets smaller the $h(p)$ values get larger.

(4) From Tables V and VI we see that as parameter μ gets smaller the corresponding eigenvalues are also smaller because the $h(p)$ values get larger as μ decreases.

These results are shown in Figs. 4–7. From them we can see that the influence of the self-energy diagrams is considerable.

V. WAVE FUNCTIONS

In Fig. 8 the dot-dash line represents the wave function $\psi^{+\prime}_{0,0}$ corrected by the self-energy diagrams ($\mu = 1, \eta = 0$). This correction diminishes the eigenvalues from $\lambda^+_{0,0} = 3.14$ to $\lambda^+_{0,0} = 2.01$. However, it can be seen from Fig. 8 that the correction to the shape of the wave function is small. Moreover, this correction becomes smaller as η increases. For $\eta = 0.99$ (Fig. 9) $\psi^{\prime+}_{0,0}$ with the contribution from the self-energy diagrams and $\psi^+_{0,0}$ without the self-energy diagrams are nearly the same. The effect of the self-energy diagrams on the shape of the wave functions is much smaller for the ground state of the symmetric case.

Figure 10 represents the antisymmetric wave function $\psi^-_{0,0}$ of the ground state without considering the effect of the self-energy diagrams ($\mu = 1$, $\eta = 0$). The behavior of the wave functions is very smooth. We cannot find any strange behavior comparing it with the wave function $\psi^+_{0,0}$.

Figure 11 represents the eigenvector $\chi^-_{0,0}$ (Fig. 10) by the formula (2.13). After the correction by the self-energy diagrams, $\chi^-_{0,0}$ changes into a δ-function-like solution, as shown in the upper right corner of Fig. 11. The central position of $\chi^-_{0,0}$ is just where $h(p)$ takes the maximum. In this case the self-energy diagrams are dominant in the equation.

VI. CONCLUSION

As $\eta \to 1$ the eigenvalues λ approach the same limit in the cases without self-energy diagrams

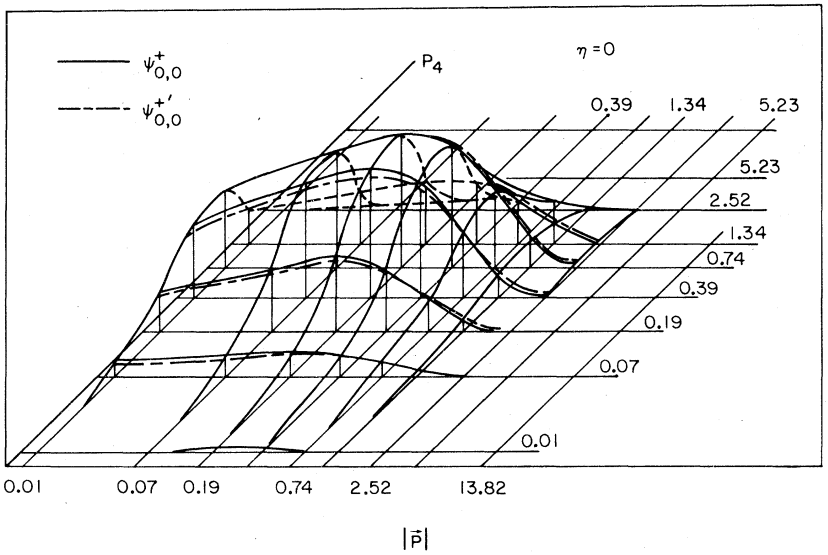

FIG. 8. Wave functions $\psi^+_{0,0}$ and $\psi^{+\prime}_{0,0}$ at $\eta = 0$ and $\mu = 1$.

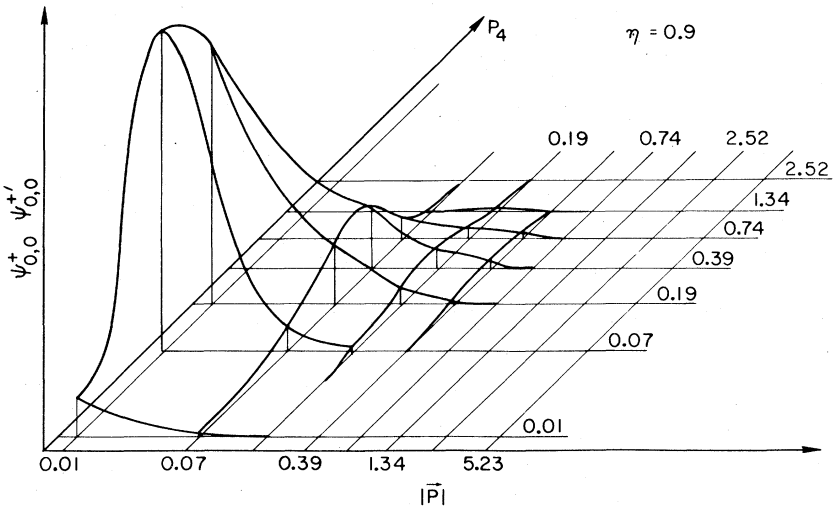

FIG. 9. Wave functions $\psi^{+}_{0,0}$ and $\psi^{+'}_{0,0}$ at $\eta = 0.99$ and $\mu = 1$.

and in those with self-energy diagrams for the symmetric ground state. The self-energy diagrams are not important for the loosely bound state and the ladder approximation is better in this case.

The influence of the self-energy diagrams on the shape of the wave function of the symmetric ground state is small, but the influence on the eigenvalues of the symmetric ground state is large in a tight-binding region.

The influence of the self-energy diagrams on the abnormal states and excited states is very large. Their eigenvalues are independent of η and the state's quantum number. The wave function looks like a δ function. In configuration space such distributions cannot correspond to a normal bound state.

The parameter μ is related to the infrared behavior of the self-energy diagrams. As μ decreases, the contribution of the self-energy diagrams increases. For $\mu = 1$ there exists a symmetric ground state in all η values, but for $\mu = 0.1$ and 0.01 it is only when $\eta > 0.99$ that the symmetric ground state exists.

The equation without self-energy diagrams is a standard Fredholm integral equation, but the equation with self-energy diagrams is not. The general BS equation can be written as

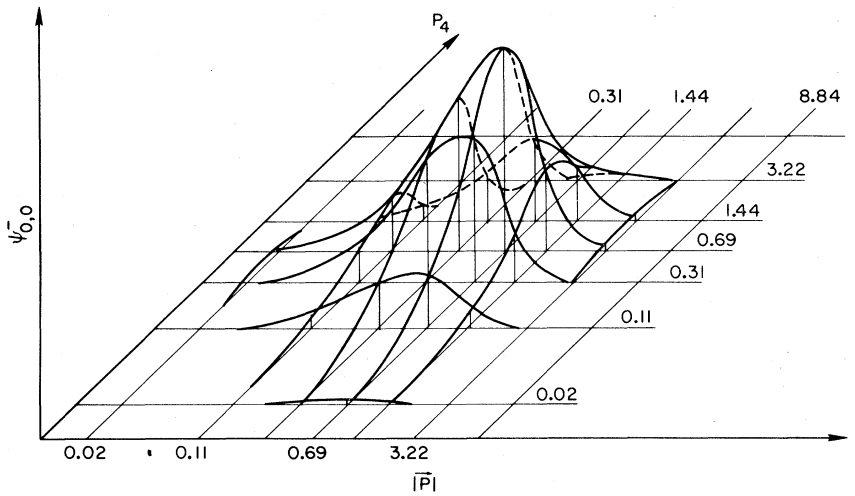

FIG. 10. Wave function $\psi^{-}_{0,0}$ at $\eta = 0$ and $\mu = 1$.

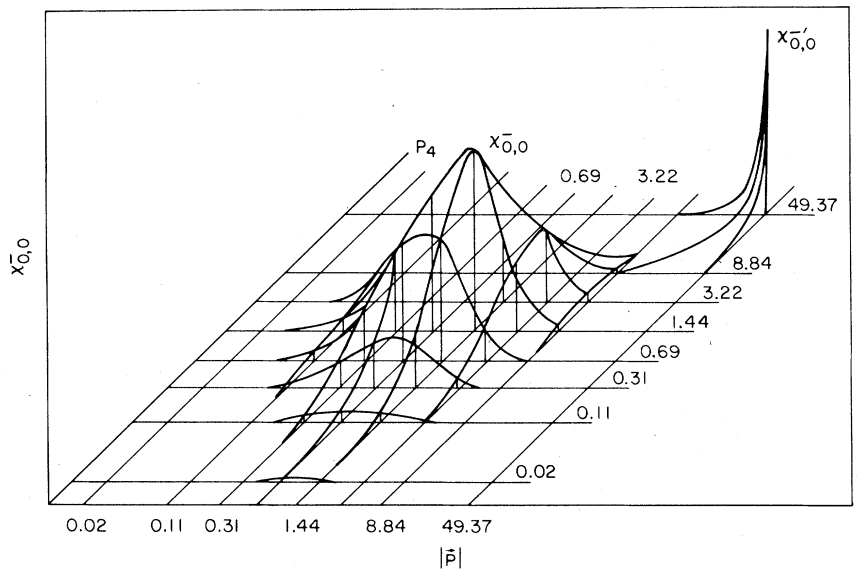

FIG. 11. Wave function $\chi_{0,0}^{-}$ and $\chi_{0,0}^{-\prime}$ at $\eta = 0$ and $\mu = 1$.

$$\chi(p) = A(p)\chi(p) + \int G(P,p,p')\chi(p')d^4p'. \qquad (6.1)$$

The function $A(p)$ denotes the contribution of all the self-energy diagrams and G denotes all the four-point irreducible Feynman diagrams. In this paper only the simplest case is discussed. In general, the equation is very complicated. However, the results obtained by us show that the balance between the two terms is needed in order to obtain a physical solution. In the configuration space the term of the self-energy diagrams represents the nonlocal interaction. In the case of the strong interaction the nonlocal interaction is important.

ACKNOWLEDGMENTS

We would like to thank Professor S. Drell, R. Blankenbecler, Y.S. Tsai, and Dr. Bing-ren Li for their helpful discussions. This work was supported in part by the Department of Energy under Contract No. DE-AC03-76SF00515 and by the People's Republic of China.

*On leave of absence from the Institute of High Energy Physics, Beijing, People's Republic of China.

[1]G. C. Wick, Phys. Rev. 96, 1124 (1954).
[2]R. E. Cutkosky, Phys. Rev. 96, 1135 (1954).
[3]Noboru Nakanishi, Prog. Theor. Phys. Suppl. 43, 1 (1969).
[4]R. Blankenbecler and R. Sugar, Phys. Rev. 142, 1051 (1966).
[5]M. J. Levine and Jan Wright, Phys. Rev. 154, 1433 (1967).
[6]M. J. Levine and Jan Wright, Phys. Rev. 157, 1416 (1967).
[7]E. Zur Linden and H. Mitter, Nuovo Cimento 61B, 389 (1969).
[8]A. Pagnamenta, Nuovo Cimento 53, 30 (1968).
[9]Charles Schwartz, Phys. Rev. 137, 717 (1965).